A Small Molecule Modulating Monounsaturated Fatty Acids and Wnt Signaling Confers Maintenance to Induced Pluripotent Stem Cells Against Endodermal Differentiation

Vahid Hosseini (Hosseiniv@tbzmed.ac.ir)
Tabriz University of Medical Sciences https://orcid.org/0000-0002-1422-2355
Ashkan Kalantary-Charvadeh
Hamadan University of Medical Sciences
Maryam Hajikarami
Royan Institute
Parisa Fayyazpour
Tabriz Medical University: Tabriz University of Medical Sciences
Reza Rahbarghazi
Tabriz University of Medical Sciences
Mehdi Totonchi
Tabriz University of Medical Sciences
Masoud Darabi
Tabriz University of Medical Sciences

Research Article

Keywords: Germ layers, Desaturation, Pluripotent stem Cells, Post-translational modification, Wnt signaling pathway, Wnt3a protein

Posted Date: August 6th, 2021

DOI: https://doi.org/10.21203/rs.3.rs-764231/v1

Version of Record: A version of this preprint was published at Stem Cell Research & Therapy on October 21st, 2021. See the published version at https://doi.org/10.1186/s13287-021-02617-x.

Abstract

Background: Stearoyl-coenzyme A desaturase 1 (SCD1) is required for *de novo* synthesis of fatty acids. This enzyme can orchestrate posttranslational modification of proteins involved in the development and differentiation of cells through the fatty acid acylation process. In this study, we evaluated whether a small molecule modulating unsaturated fatty acids influences early endodermal differentiation of induced pluripotent stem cells, using biochemical methods and immunostaining.

Methods: The hiPSCs were cultured in an endoderm-inducing medium containing activin A and low defined fetal bovine serum in the presence of an SCD1 inhibitor at different time points. The yield of three germ layers endoderm, mesoderm, and ectoderm, and the cell cycle analysis were assessed using flow cytometry. The expression of endoderm and pluripotency markers, as well as the expression of Wnt signaling pathway proteins, were assessed using western blotting and RT-PCR. Total protein acylation was evaluated using a click chemistry reaction.

Results: The population of cells showing endoderm features was decreased at the end of differentiation when SCD1 was inhibited on the first day. Moreover, early SCD1 inhibition preserved hiPSCs properties without a shift toward mesoderm or ectoderm. Treatment of cells with SCD1 inhibitor only on the first day decreased the β-catenin gene expression and intensity of fluorescent emission in the click chemistry. These effects were effectively rescued by cotreatment with oleate. Late treatment at two subsequent days of endoderm induction induced no significant effect on endoderm-specific markers and fluorescent intensity. Reproducible results were also obtained with a human embryonic stem cell line.

Conclusion: The small molecule SCD1 inhibitor attenuates the Wnt/β-catenin signaling pathway, conferring maintenance to hiPSCs by opposing the initiation of endoderm differentiation. The immediate requirement for SCD1 activity in endoderm commitment of pluripotent stem cells may be eminent in disorders of endoderm-derived organs and dysregulated metabolism.

2. Introduction

Human-induced pluripotent stem cells (hiPSCs) are directly generated from adult somatic cells by reprogramming procedure. It was suggested that hiPSCs have a great potential to commit into endodermal, mesodermal, and ectodermal cell lineages (1). The existence of unique pluripotency, high proliferation rate, lack of unwanted immunological reactions, and ethical concerns make hiPSCs valuable biological tools in the regenerative medicine area (2). Besides, hiPSCs can also be used in various fields of biomedical science, including drug screening, finding the genetic basis of diseases, and investigation of molecular mechanisms regulating differentiation (3–6).

Monounsaturated fatty acids (MUFAs) are essential precursors for building cell structure and bioactive lipids (7). Of note, endoplasmic reticulum enzyme namely Stearoyl-coenzyme A desaturase 1 (SCD1) promotes the synthesis of MUFAs by adding a double bond between carbon 9 and 10 of saturated fatty acids (SFAs), hence regulating the ratio of MUFAs to SFAs in cells (8, 9). Wnt ligand proteins are the most

well-known biomolecules undergoing post-translational modification with MUFAs through Porcupine (Porcn) catalytic activity which appends MUFAs particularly palmitoleate on Ser209 residue of Wnt proteins (10). It has been indicated that there is a close association between Wnt proteins and MUFAs. For instance, Wnt protein activation, intra-, and extra-cellular transportation, and binding to cell surface receptors are dependent on MUFA residue. In human embryonic stem cells (hESCs) and mouse induced pluripotent stem cells (miPSCs), the activity of SCD1 supports cell growth and survival (11). The *in vitro* suppression of SCD1 can lead to selective elimination of pluripotent cells (12). Interestingly, the injection of miPSCs and hESCs pre-treated with an SCD1 inhibitor reduced the anaplastic changes and teratoma formation in immunosuppressed mice. Additionally, this strategy can improve stem cell safety after cardiac transplantation (12, 13). As a correlate, these findings confirm the crucial role of SCD1 in stem cell bioactivity and functional fate acquisition. High intracellular rates of SCD1 have been reported in endoderm-derived tissues such as the liver and pancreas. Similarly, SCD1 content is also relatively high in some non-endodermal tissues such as adipose tissue, indicating tissue-and lineage-dependent activity of SCD1 (14, 15). Noteworthy, SCD1 activity in stem cells is relevant to the characteristics of adipogenic differentiation (16). Previously, our research group showed the importance of SCD1 products in hepatic differentiation of hiPSCs (17) coincided with *in vivo* data (18). Commensurate with these findings, one could suggest that SCD1 products not only can enter the metabolic pathways but are also potentially involved in signaling pathways related to cell differentiation.

There is no report as yet assessing the kinetic effect of the small molecules targeting SCD1 during endodermal differentiation of pluripotent stem cells. In this study, we evaluated whether the dynamic of SCD1 activity is important in the differentiation of hiPSCs to endoderm lineage using biochemical methods, acylation assay, and immunostaining. According to the results, small molecule SCD1 inhibitors can support hiPSCs maintenance by postponing the endoderm differentiation.

3. Materials And Methods

3.1. Materials

All cell culture materials were obtained from Gibco (USA) unless otherwise specified.

3.2. Primary mouse embryonic fibroblasts (MEFs) isolation

Primary MEFs were isolated by a mechanical technique and characterized as described by our previous study (19). In short, embryonic fibroblasts with the passage number 1–5 were commonly proliferated in a culture flask pre-coated with 0.2% gelatin (Sigma, Germany) containing 10 ml of Dulbecco's minimum eagle's medium (DMEM; Gibco, USA) and 10% fetal bovine serum (FBS). Before stem cell culture, MEF were treated with 10 µg/ml Mitomycin C (Abcam, UK) for 3 hours to inhibit cell proliferation.

3.3. Stem cell culture and expansion

The established normal R1-hiPSC and hESC XX Royan H1 cell lines (20) were used in this study. The pluripotent stem cells (PSCs) culture media was composed of 75% DMEM/F12 supplemented with 20%

knockout serum replacement, 1% non-essential amino acids, 2 mM L-glutamine (Sigma, Germany), 0.1% β-mercaptoethanol (Merk, Germany), 1% insulin/transferrin/selenium solution, and 12 ng/ml basic human recombinant FGF (b-FGF) (Royan, Iran). The standard cultures were split at the ratio of 1:5 every 7–10 days.

3.4. Endoderm differentiation

Upon 70–80 confluence, hiPSCs were detached using 1 mg/ml Collagenase Type IV (Stem Cell Technologies, Canada) and dissociated into single cells by gentle pipetting. The cells were washed with phosphate-buffered saline (PBS) and suspended in fresh ESCs culture media containing 100 ng/ml of b-FGF, and then transferred on Matrigel- (Sigma, Germany) coated 60 mm plates. The next day, the medium was discarded and the differentiation medium consisted of RPMI-1640 with 100 ng/ml activin A (BioLegend, USA) with varying concentrations of defined-FBS (D-FBS) used. The concentrations of D-FBS were set to 0% (Day 0), 0.2% (Day 1), and 2% (Day 2 and 3).. The cells were harvested and used for different analyses at the fourth 24h (Day 4) (21).

3.5. Targeting SCD1 by small molecule inhibitor

Chemical inhibition of SCD1 was performed with the specific inhibitor of SCD1 CAY10566 (Cayman Chemical, USA). Cells were treated with SCD1 inhibitor for 24 hours at days 0, 1, or 2 of the differentiation procedure. In our previous study, the possible toxicity of the inhibitor was determined using Trypan Blue exclusion and sulforhodamine B assays after treatment with 25 nmol/L CAY10566 or lower concentrations (17). The rescue experiments were performed using 50 μM oleate.

3.6. Evaluation of cell viability

An Annexin V-FITC/PI apoptosis detection kit (eBioscience, USA) was used for the apoptosis analysis. After completion of the endodermal differentiation procedure, cells were detached with collagenase IV and washed once with PBS. The cells were suspended in the binding buffer (1X), incubated with 5 μl Annexin-V for 10 minutes, and washed once with binding buffer. The cells were re-suspended again in 200 μl of binding buffer followed by the addition of 10 μl of propidium iodide. The percentage of apoptosis and necrosis was determined using a flow cytometer (Miltenyi Biotec, USA) and results were analyzed using flow Jo 7.6.1 software (Tree Star, USA).

3.7. Morphological examination

The morphological alteration was visually monitored using a Cytation 5 Cell Imaging Multi-Mode Reader system (BioTek, USA). Differentiating cells were imaged every 24 hours for consecutive 4 days in the absence or the presence of CAY10566.

3.8. Gene expression assay

Total RNA extraction was carried out using an RNA extraction kit (TaKaRa, Japan) following the instructions provided by the manufacturer. The quantity and quality of extracted RNA were checked using a spectrophotometer (NanoDrop Technologies, USA) and running on 1.5% agarose gel, respectively. The

complementary DNA (cDNA) required for real-time PCR was synthesized with a cDNA synthesis kit (Roche, UK). Real-time PCR was performed with SYBR Green PCR master mix (Yekta Tajhiz Azma, Iran) on a MIC real-time PCR system (BioMolecular Systems, Australia). The primer sequences used for Sox2, Oct4, Sox17, and CXCR4 expression assay are listed in Supplementary Table 1. Relative gene expression was normalized against the expression level of GAPDH as a reference gene for each sample and all alterations were expressed as fold-changes relative to the mock.

3.9. Surface markers analysis

The pellet of disassociated cells was resuspended in 4% paraformaldehyde to fix the cells by a 30 minutes incubation at 4°C. Cells were then resuspended in PBS containing 1% BSA as a staining buffer and incubated for 20 minutes at 4°C. Then, cells were incubated with Alexa Fluor 488-conjugated CXCR4 (R&D, USA) and PE-conjugated KDR (R&D, USA), Alexa Fluor 488-conjugated SSEA-3, (eBioscience, USA), or PE-conjugated NCAM antibodies at 4°C for 1 hour. After PBS washes, cells were analyzed using a flow cytometer (Miltenyi Biotec, USA) and the data were analyzed by the Flowing Software 2.5.1 (Turku Bioscience, Finland).

3.10. Western blotting

The cell lysate from each group was prepared using a RIPA lysis buffer containing protease inhibitor. Samples were centrifuged and the total protein concentration of supernatants determined by Lowry protein assay. Twenty µg of protein was mixed with an equal volume of sample buffer and electrophoresed on SDS-PAGE, then transferred onto PVDF membranes (Santa Cruz, USA). After blocking with 5% skimmed milk, the membrane was washed in PBS with Tween detergent and treated with primary antibodies against the pluripotency markers Oct4 (Abcam, USA) and Sox2 (Abcam, UK), endodermic markers CXCR4 (Santa Cruz, USA) and Sox17 (Santa Cruz, USA), and the internal control β-actin (Santa Cruz Biotechnology, USA) overnight at 4°C. Primary antibodies against Wnt3a (Santa Cruz, USA) and β-catenin (Santa Cruz) were applied for evaluation of Wnt signaling pathway. Then, the membrane was exposed to horseradish peroxidase (HRP)-conjugated secondary antibody for 1 hour at RT. Finally, the membrane was visualized by luminol reagents (Santa Cruz, USA). The intensity of the bands was quantified using ImageJ software (version 1.41).

3.11 Cell proliferation assay

The proliferation rate was measured using a 5-bromo-2-deoxyuridine (BrdU) assay (Abcam, USA). To this end, cells were seeded at a density of 2×10^4 cells per well of 96-well plates. After completion of the treatment protocol, each well was filled with BrdU reagent before cell harvesting. Cellular DNA was denatured with the fixing solution at RT. After washing with PBS, the anti-BrdU monoclonal antibody was added to each well, and plates were incubated for 1 hour at RT. Then, supernatants were discarded and the washing step was repeated followed by the addition of an HRP-conjugated anti-IgG antibody. After the final wash, each well was incubated with a peroxidase substrate and then the reaction was stopped by adding the stop solution when the yellow color was generated. The optical density of the solution was

measured using a microplate reader (Labsystems, Finland) at 450 nm. Wells containing media alone and seeded cells without BrdU reagent were used as blank and background controls, respectively.

3.12 Acylation assay

In order to evaluate the total protein acylation, we performed an Alkyne-azide cycloaddition click reaction according to a standard protocol (22). Briefly, cells were seeded onto a 24-well plate at a density of 5×10^4 cell/well and treated as abovementioned. Medium containing the ω-alkynyl analog of palmitic acid (Alk-C16) was added into the wells at each time point after washing once with PBS and incubated for 24 hours at 37°C with 5% CO_2 to label the cells. After discarding the medium, cells were then washed with pre-cooled PBS, fixed with − 20°C pre-chilled methanol. Permeabilization was performed using Triton X-100 at RT for 5 minutes. Cells were washed with PBS and exposed to a click labeling reagent containing Alexa Fluor 488 Azide (Invitrogen, USA), Tris (2-carboxyethyl) phosphine hydrochloride (TCEP) (Cayman, USA), and $CuSO_4$ for 1 hour at RT and dark. The wells were then washed with PBS, incubated with 4',6-diamidino-2-phenylindole (DAPI) for 30 S at RT, and washed three times with PBS. Finally, cells were imaged using the cell imaging system at excitation 488/emission 516 nm for Alexa Fluor488 and excitation 377/emission 477 nm for DAPI.

3.13 Cell cycle analysis

Cell cycle assay was performed using a cell cycle phase determination kit (Cayman Chemical, USA). Cells were seeded on the culture plates according to the manufacturers' instructions. After completion of treatment protocols, the cells were trypsinized, centrifuged, and washed with the assay buffer. The cell pellet was resuspended in the assay buffer and incubated with a fixation buffer. Then, the cell suspension was centrifuged and the supernatant was discarded followed by incubation in staining solution at RT and dark. The percentage of cells in each phase was determined using Flowing software 2.5.1 (Turku Centre for Biotechnology, Finland).

3.14 Statistical Analysis

Experimental data are presented as mean ± standard deviation (SD) of the mean from at least three independent experiments. One-way or two-way analysis of variance (ANOVA) followed by Turkey’s post-hoc test was applied for Groupwise comparisons (GraphPad Software 8.0, USA). A p-value less than 0.05 was considered to be significant.

4. Results

4.1. SCD1 inhibition did not affect cell viability and proliferation

In order to evaluate the toxic effect of inhibitor concentration on stem cell viability and proliferation, hiPSCs and ESCs were treated with inhibitor at day 0 during endoderm differentiation. The flow cytometry results demonstrated that the applied concentration of SCD1 inhibitor did not induce an apoptotic or necrotic effect on cells and the majority of cells were Annexin-V and PI negative (Fig. 1). Similarly, the cell proliferation rate was also not altered after inhibition of SCD1 at days 0, 1, or 2 during endoderm differentiation compared to the mock group ($p > 0.05$). According to our data, the proliferation rate was high in which more than 70% of cells were BrdU positive at day 4 of differentiation (Fig. 2).

4.2. SCD1 inhibition maintained stem cell features

Bright-field microscopic imaging displayed prominent morphological changes during endoderm induction (**Figure. S1**). One day after differentiation protocol, cells lost typical morphological characteristics, i.e. round and compact cells with high nuclear/cytoplasm ratio, and morphologically different cells appeared. Following the next days, the number of morphologically different cells was increased. On day 5, a monolayer of morphologically uniform cells with petal/cobblestone-like morphology and optically clear cytoplasm were obtained (**Figure S1**). We showed that stem cell morphology was unchanged only at day 0 of SCD1 inhibition. Noteworthy, co-treatment of cells with oleate can change morphological features (Fig. 3).

4.3. SCD1 inhibition reduced the expression of endodermal markers

In differentiated cells, the expression rate of the endodermal markers Sox17 and CXCR4 was robustly elevated coincided with down-regulation of pluripotency markers Oct4 and Sox2 (Fig. 4), indicating the efficiency of the current protocol to commit the cells toward an endoderm-like cell population. To examine the effect of SCD1 inhibition on differentiation of hiPSCs toward endodermal lineage, one-shot treatment of cells with a non-toxic concentration of SCD1 inhibitor was performed at day 0, day 1, and day 2 of the differentiation process. The alterations of pluripotency and endodermal markers were assessed at both gene and protein levels. Briefly, the inhibition of SCD1 prevented significantly the down-regulation of pluripotency markers Oct4 and Sox2 and the increase of endodermal lineage gene markers Sox17 and CXCR4 compared to the mock condition (Figs. 4 and 5). Based on our data, the effect of SCD inhibition was less at day 2 of differentiation. As indicated in Figs. 4 and 5, in undifferentiated hiPSCs the expression of the stemness marker Oct4 were 21.39-fold (gene, $p < 0.01$) and 3.67-fold (protein, $p < 0.01$) whereas these values were 16.01 ($p < 0.01$) and 3.2 ($p < 0.01$) for Sox2. According to our data, the both transcription and protein levels of CXCR4 and Sox17 reached to 0.04- (gene, $p < 0.01$), 0.22- (protein, $p < 0.01$), 0.04- (gene, $p < 0.01$) and 0.17-($p < 0.01$) folds compared the mock group.

In differentiated cells, the transcription and protein levels of Oct4 were 13.02 (gene, $p < 0.01$) and 2.88 (protein, $p < 0.01$) fold, respectively. Of note, the values for Sox2 were 9.63- (gene, $p < 0.01$) and 2.76 (protein, $p < 0.05$) fold higher compared to the mock when SCD1 inhibited at day 0. We noted that the expression of stemness markers was not significantly altered when SCD1 was inhibited at day 1, except for Sox2 which was 6.2-fold (gene, $p < 0.01$) higher in comparison to mock. In differentiated cells, the

expression of endoderm markers CXCR4 was 0.39- (gene, $p < 0.01$) and 0.27- (protein, $p < 0.01$) fold. The expression of Sox17 was 0.27- (gene, $p < 0.01$) and 0.24- (protein, $p < 0.01$) fold compared to the mock group when SCD1 was inhibited at day 0 (Figs. 4 and 5). Data showed that endodermal markers revealed that only the transcription of Sox17 was 0.43-fold (gene, $p < 0.01$) at day 1 compared to the mock group. The ESCs demonstrated a similar pattern of results after the inhibition of SCD1 during endodermal inhibition. As expected, in the rescue experiment, using oleate together with SCD1 inhibitor, the expression of endoderm markers was efficiently recovered (Figs. 4 and 5).

4.4. SCD1 inhibition did not divert differentiation of hiPSCs toward mesodermal or ectodermal lineages

A combination of surface markers, representing all three germ layer cells and undifferentiated cells, was analyzed to distinguish each cell type upon SCD1 inhibition and endodermal differentiation. We found that the percentage of endoderm cells was decreased 2.56 fold ($p < 0.01$) with the inhibition of SCD1. Interestingly, The percentage of undifferentiated cells in the mock group was increased 8.2 fold ($p < 0.01$) and 2.49 fold ($p < 0.05$) following the inhibition of SCD1 at days 0 and 1, respectively. With the addition of oleate together with SCD1 inhibitor at day 0, the percentage of endoderm cells and undifferentiated cells were increased 2.4 fold ($p < 0.01$) and decreased to 6.53 fold ($p < 0.01$) compared the same day without the presence of SCD1 inhibitor, respectively. Notably, inhibition of SCD1 did not significantly alter the percentage of the ectoderm or mesoderm population (Fig. 5).

4.5. SCD1 inhibition resulted in a decrease in total protein acylation

In order to evaluate the effect of SCD1 inhibition on the acylation of total proteins during endoderm induction, the total protein acylation rate of pluripotent stem cells was measured using click chemistry. Fluorescent imaging results demonstrated a high and constant acylation rate during normal endoderm differentiation (**Figure S2**). However, the inhibition of SCD1 activity at days 0, 1, or 2 decreased the intensity of the fluorescent emission, which was significant on day 0. In particular, the emission intensity reached 0.59- ($p < 0.05$) and 0.67- ($p < 0.05$) fold compared to the mock group after the inhibition of SCD1 at day 0 in hiPSCs (Fig. 6A-B) and ESCs (Fig. 6C-D), respectively. A decrease in the fluorescent emission was also observed at day 1 after treatment with SCD1 inhibitor (0.63-fold of mock, $p < 0.05$, Fig. 6A-B).

4.6. SCD1 inhibition increased the percent of cells in the S phase

The distribution of differentiated hiPSCs in cell cycle phases was determined using single color flow cytometry analysis after DNA staining with PI. In the undifferentiated cells, the percentage of cells in the G1 and S phases was 19.14 and 56.04, respectively, showing the characteristics of PSCs (Fig. 7). In this condition, the percentage of cells in G1 and S phases was 0.53- ($p < 0.01$) and 1.5- ($p < 0.01$) fold of the mock group, respectively. The inhibition of SCD1 activity reduced the percentage of cells in the G1 phase (0.58-fold, $p < 0.05$) at day 0 and concomitantly increased the percentage of cells in the S phase (1.52-

fold, $p < 0.01$) as compared to the mock group. In the rescue experiment, the percentage of cells in the G1 and S phases were close to the mock condition. The percentage of cells in G1 and S phases were increased 1.74 and decreased 0.69-fold, respectively compared to time-matched groups that received SCD1 inhibitor (Fig. 7).

4.7. Inhibition of SCD1 decreased endoderm differentiation through attenuation of Wnt signaling pathway

Western blotting showed that the protein levels of Wnt3a and its downstream β-catenin were gradually decreased from day 0 to day 4 during endoderm differentiation (**Figure S3**). Data showed the lack of significant difference in the expression of β-catenin following the inhibition of SCD1 at days 0, 1, or 2 of differentiation. Upon SCD1 inhibition at day 0, the expression of Wnt3a was 1.57- and 1.26-fold higher than that of values observed in the same days without the inhibition of SCD1 ($p < 0.05$). As expected, the addition of oleate at the same time efficiently counteracted the increasing and decreasing effects of the inhibitor on Wnt3a and β-catenin, respectively (Fig. 8).

5. Discussion

PSCs with a high potential to differentiate into adult functional cells are promising options for the treatment of human degenerative diseases (23). The application of these cells in the clinical setting is mainly hindered by their low differentiation efficiency of *in vitro* protocols and the possibility of tumorigenicity after transplantation into the target organs (24, 25). In addition, the self-differentiation of these cells during expansion steps makes the handling of these cells more difficult. Commensurate with these comments, the subtle and precise control of differentiation is critical to overcoming this challenge. The increasing knowledge of molecular mechanisms governing cell differentiation will help us to provide an optimum condition for differentiation and maintenance of stem cell behavior either preclinical models or in clinical applications.

MUFAs play important roles in developmental processes through post-translational modification of proteins involved in differentiation. Therefore, understanding the mechanisms by which MUFAs metabolism affects stem cell behavior offers promising perspectives to regulate pharmacologically stem cell differentiation. In the current study, we evaluated the effect of SCD1 inhibition on endodermal differentiation in PSCs by monitoring the protein and transcription levels of molecular markers, total protein acylation, cell viability, cell proliferation, cell cycle, and Wnt signaling pathway. To assess the specificity of effects, the main product of SCD1 oleate was co-administrated with the chemical inhibitor.

We observed no significant changes in the PSC proliferation, apoptosis, and necrosis rates after SCD1 inhibition compared to the control group. Therefore, it seems that SCD1 inhibition affects the PSCs independent from cell proliferation, apoptosis, or necrosis. Consistent with our data, the inhibition of SCD1 with similar concentrations of inhibitor did not alter cell viability during liver differentiation of hiPSCs (17). However, treatment of ESCs-derived endoderm progenitor cells, ESCs-derived hepatocytes, and iPSCs-derived cardiomyocytes with the toxic concentration of SCD1 inhibitor was shown to

selectively eliminate the cells at undifferentiated staus (12). Of note, the incubation of lung cancer cells with the SCD1 inhibitor induced toxicity in cancer stem cells (26). These findings report that the inhibition of SCD1 in different progenitor lineages can yield different outcomes in dynamic growth. The exact mechanism and underlying machinery participating in this phenomenon are lacking. Our findings showed that the inhibition of SCD1 can reduce the PSC differentiation capacity toward endodermal lineage while maintained pluripotency of the cells. It confirmed that the efficiency of the SCD1 inhibition did vary with time during endoderm differentiation. Following the inhibition of SCD1 at day 0 of differentiation, the synthesis of endoderm markers was markedly suppressed. As expected, treatment of cells with SCD1 inhibitor together with exogenous oleate recovered these effects. The precise cellular mechanism supports these effects is that palmitoleate is also the product of SCD1 like oleate. It seems that oleate alone could compensate the deficiency of SCD1 activity during endoderm differentiation of PSCs. In line with our study, the suppression of SCD1 activity during hepatic differentiation of delayed the production of hepatic function markers at liver maturation step (17). Presumably, the activity of SCD1 is reduced concomitantly by the progression of cells toward specialized cells (17). Data were further confirmed the pivotal role of SCD1 in the development of the liver in rat embryos (18). The Inhibition of SCD1 in an early phase of pregnancy led to severe defects in fetal liver development indicated by the down-regulation of HNF1α, AFP, ALB, and CYP450 (18). These effects were blunted in the presence of oleate (17, 18). It was suggested that the inhibition of Porcn, an acyltransferase catalyzing the addition of MUFAs onto Wnts, using IWP-2 reduced the expression of endoderm markers such as Sox17 and FOXa2 a few hours before initiation of endoderm induction (27). Along with our results, it can be proposed that SCD1 and its products are involved in the development and differentiation of stem cells into the endodermal lineage (28, 29). By contrast, some reports demonstrated different results associated with the function of SCD1 products in stem cells. It was recently found that after treatment of MEFs during reprogramming into iPSCs, resulted iPSCs formed more colonies in comparison to the non-treated control. These iPSCs had a higher capacity for palmitoleate and oleate synthesis. Remarkably, inhibition of Porcn can lead to a reduction of ESCs pluripotency (30). These results indicate that SCD1 can act in a context-dependent manner in terms of cell fate acquisition. The function of SCD1 can promote cell differentiation and its function is critical in early phase of differentiation. Meanwhile, it can help maintaining stem cell features. The similar effects have been reported in molecules dependent to MUFAs such as Wnt molecules. Several conflicting reports in literature show that the Wnt molecules promote either stemness or differentiation and lineage specification of stem cells (31-35).

To investigate the possible role of SCD1 in the acylation rate proteins, we used click chemistry and fluorescent imaging during endoderm differentiation and following the SCD1 inhibition. The Alk-C16 probe analysis showed that endoderm differentiation is associated with a significant protein acylation signal. This finding implies that a great deal of proteins undergoes acylation by fatty acids in stem cells subjected to endodermal differentiation. Previously, it has been shown that Alk-C16 can be converted into its monounsaturated form Alk-C16:1 by the activity of SCD1 (36). Therefore, the intensity of the signal is associated with the incorporation of both saturated and monounsaturated forms of the prob. Importantly, the acylation rate was significantly decreased when the SCD1 was inhibited on day 0. We interpreted this

event as correlates with the reduction of the monounsaturated form of Alk-C16 for incorporation and biochemical reactions.

Previous studies showed the significant role of Activin A and Wnt/β-catenin pathways in the endodermal differentiation of ESCs (27, 37, 38). Activin A-induced SCD1 can produce metabolites that can post-translationally modify the Wnt molecules (38). The contribution of SCD1 in the activity of Wnt signaling was assessed using western blotting and gene expression analysis. Results showed mild to moderate suppression of Wnt3a/β-catenin during differentiation of iPSCs toward endodermal lineage, indicating the crucial role of SCD1 in the early-stage stem cell differentiation capacity. Following the treatment of cells with the SCD1 inhibitor, the expression of Wnt was increased with non-significant changes in β-catenin. One reason related to Wnt induction would be that the expression of Wnt is a compensatory response after the suppression of MUFA acylation via SCD1 product. Additionally, the slight to mild suppression of β-catenin can be related to the attenuation of the Wnt signaling pathway following the SCD1 inhibition, these features result in reduced endoderm differentiation of iPSCs. Based on these results, we hypothesize that the changes in the Wnt/β-catenin signaling pathway are possibly due to the reduced MUFA acylation. Besides, results showed that SCD1 activity can be changed during cell differentiation. To be specific, MUFAs were much more essential at the first stages than the latter steps, indicating immediate triggering activity of SCD1 is essential for endodermal differentiation in hiPSCs. As indicated previously, the generation of the primitive streak and subsequently formation of mesodermal cells are a prerequisite for the formation of endoderm (21, 39). Most probably, MUFAs are required for the production of primitive streak- and mesendoderm-like cells, yet the hypothesis needs to be investigated in future studies.

Conclusions

Overall, the dynamic of SCD1 activity is important in the early commitment and differentiation of hiPSCs to endoderm lineage. We showed that SCD1 inhibition attenuates the Wnt/β-catenin signaling pathway, conferring maintenance to hiPSCs by opposing the initiation of endoderm differentiation. The requirement for SCD1 activity in endoderm commitment of PSCs may be eminent in disorders of endoderm-derived organs and dysregulated metabolism.

Abbreviations

SCD1: Stearoyl-coenzyme A desaturase 1

hiPSCs: Human-induced pluripotent stem cells

MUFAs: Monounsaturated fatty acids

SFAs: saturated fatty acids

hESCs: human embryonic stem cells

miPSCs: pluripotent stem cells

FBS: fetal bovine serum

b-FGF: basic human recombinant FGF

PBS: phosphate-buffered saline

D-FBS: defined-FBS

BrdU: 5-bromo-2-deoxyuridine

Alk-C16: ω-alkynyl analog of palmitic acid

TCEP: Tris (2-carboxyethyl) phosphine hydrochloride

SD: standard deviation

Declarations

Contributions

MD conceived and designed the experiments. VH performed cell isolation, and molecular analyses, and wrote the manuscript draft. VH and MH performed cell culture. AKC and PF performed extractions and blotting. MD, MT, RR, and AKC reviewed the manuscript. All authors read and approved the final manuscript.

Funding

The research protocol was approved & Supported by the Student Research Committee, Tabriz University of Medical Sciences (59924), Stem Cell Research Center, Tabriz University of Medical Sciences (65430), and the National Council for Development of Stem Cell Sciences and Technologies (394).

Ethics declarations

Ethic approval and consent to participate

The study protocols were approved by the Tabriz University of Medical Sciences Ethics Committee (IR.TBZMED.REC.1395.680). All animals were treated according to guidelines for the Care and Use of Laboratory Animals (NIH; 1986).

Consent for publication

Not applicable

Competing interests

The authors declare that they have no competing interests.

Availability of data and materials

Not applicable

References

1. Yu J, Vodyanik MA, Smuga-Otto K, Antosiewicz-Bourget J, Frane JL, Tian S, et al. Induced pluripotent stem cell lines derived from human somatic cells. science. 2007;318(5858):1917–20.
2. Yamanaka S. Induced pluripotent stem cells: past, present, and future. Cell stem cell. 2012;10(6):678–84.
3. Liu G, David BT, Trawczynski M, Fessler RG. Advances in pluripotent stem cells: history, mechanisms, technologies, and applications. Stem cell reviews reports. 2020;16(1):3–32.
4. Rowe RG, Daley GQ. Induced pluripotent stem cells in disease modelling and drug discovery. Nat Rev Genet. 2019;20(7):377–88.
5. Hirabayashi M, Goto T, Hochi S. Pluripotent stem cell-derived organogenesis in the rat model system. Transgenic research. 2019:1–11.
6. Hosseini V, Maroufi NF, Saghati S, Asadi N, Darabi M, Ahmad SNS, et al. Current progress in hepatic tissue regeneration by tissue engineering. Journal of translational medicine. 2019;17(1):383.
7. Nagy K, Tiuca I-D. Importance of fatty acids in physiopathology of human body. Fatty acids: IntechOpen; 2017.
8. Ntambi J. Dietary regulation of stearoyl-CoA desaturase 1 gene expression in mouse liver. J Biol Chem. 1992;267(15):10925–30.
9. Mohammadzadeh F, Hosseini V, Alihemmati A, Mehdizadeh A, Shaaker M, Mosayyebi G, et al. The Role of Stearoyl-coenzyme A Desaturase 1 in Liver Development, Function, and Pathogenesis. Journal of Renal Hepatic Disorders. 2019;3(1):15–22.
10. Kalantary-Charvadeh A, Hosseini V, Mehdizadeh A, Darabi M. Application of porcupine inhibitors in stem cell fate determination. Chem Biol Drug Des. 2020;96(4):1052–68.
11. Fathi Maroufi N, Hasegawa K, Vahedian V, Nazari Soltan Ahmad S, Zarebkohan A, Miresmaeili Mazrakhondi SA, et al. A glimpse into molecular mechanisms of embryonic stem cells pluripotency: Current status and future perspective. Journal of Cellular Physiology. 2020.

12. Ben-David U, Gan Q-F, Golan-Lev T, Arora P, Yanuka O, Oren YS, et al. Selective elimination of human pluripotent stem cells by an oleate synthesis inhibitor discovered in a high-throughput screen. Cell stem cell. 2013;12(2):167–79.
13. Zhang L, Pan Y, Qin G, Chen L, Chatterjee T, Weintraub N, et al. Inhibition of stearoyl-coA desaturase selectively eliminates tumorigenic Nanog-positive cells: improving the safety of iPS cell transplantation to myocardium. Cell Cycle. 2014;13(5):762–71.
14. Janikiewicz J, Hanzelka K, Dziewulska A, Kozinski K, Dobrzyn P, Bernas T, et al. Inhibition of SCD1 impairs palmitate-derived autophagy at the step of autophagosome-lysosome fusion in pancreatic β-cells. Journal of lipid research. 2015;56(10):1901–11.
15. Ntambi JM, Miyazaki M. Regulation of stearoyl-CoA desaturases and role in metabolism. Progress in lipid research. 2004;43(2):91–104.
16. Ralston JC, Mutch DM. SCD1 inhibition during 3T3-L1 adipocyte differentiation remodels triacylglycerol, diacylglycerol and phospholipid fatty acid composition. Prostaglandins Leukot Essent Fatty Acids. 2015;98:29–37.
17. Rahimi Y, Mehdizadeh A, Nozad Charoudeh H, Nouri M, Valaei K, Fayezi S, et al. Hepatocyte differentiation of human induced pluripotent stem cells is modulated by stearoyl-CoA desaturase 1 activity. Development growth differentiation. 2015;57(9):667–74.
18. Mohammadzadeh F, Alihemmati A, Tazehkand AP, Darabi M, Mehdizadeh A. Early oleate deficiency leads to severe defects in fetal rat liver development. Iranian Journal of Basic Medical Sciences. 2019;22(9):1010.
19. Hosseini V, Kalantary-Charvadeh A, Hasegawa K, Ahmad SNS, Rahbarghazi R, Mahdizadeh A, et al. A mechanical non-enzymatic method for isolation of mouse embryonic fibroblasts. Molecular Biology Reports. 2020:1–10.
20. Baharvand H, Ashtiani SK, Taee A, Massumi M, Valojerdi MR, Yazdi PE, et al. Generation of new human embryonic stem cell lines with diploid and triploid karyotypes. Dev Growth Differ. 2006;48(2):117–28.
21. D'Amour KA, Agulnick AD, Eliazer S, Kelly OG, Kroon E, Baetge EE. Efficient differentiation of human embryonic stem cells to definitive endoderm. Nature biotechnology. 2005;23(12):1534–41.
22. Gao X, Hannoush RN. Single-cell in situ imaging of palmitoylation in fatty-acylated proteins. Nature protocols. 2014;9(11):2607.
23. Trounson A, DeWitt ND. Pluripotent stem cells progressing to the clinic. Nature reviews Molecular cell biology. 2016;17(3):194–200.
24. Deng J, Zhang Y, Xie Y, Zhang L, Tang P. Cell transplantation for spinal cord injury: tumorigenicity of induced pluripotent stem cell-derived neural stem/progenitor cells. Stem Cells International. 2018;2018.
25. Singh VK, Kalsan M, Kumar N, Saini A, Chandra R. Induced pluripotent stem cells: applications in regenerative medicine, disease modeling, and drug discovery. Frontiers in cell developmental biology. 2015;3:2.

26. Pisanu ME, Noto A, De Vitis C, Morrone S, Scognamiglio G, Botti G, et al. Blockade of Stearoyl-CoA-desaturase 1 activity reverts resistance to cisplatin in lung cancer stem cells. Cancer letters. 2017;406:93–104.
27. Xu H, Tsang KS, Wang Y, Chan JC, Xu G, Gao W-Q. Unfolded protein response is required for the definitive endodermal specification of mouse embryonic stem cells via Smad2 and β-catenin signaling. J Biol Chem. 2014;289(38):26290–301.
28. Lee H, Lim J-Y, Choi S-J. Role of l-carnitine and oleate in myogenic differentiation: implications for myofiber regeneration. J Exerc Nutr Biochem. 2018;22(2):36.
29. Briolay A, Jaafar R, Nemoz G, Bessueille L. Myogenic differentiation and lipid-raft composition of L6 skeletal muscle cells are modulated by PUFAs. Biochimica et Biophysica Acta (BBA)-Biomembranes. 2013;1828(2):602–13.
30. Fernandez A, Huggins IJ, Perna L, Brafman D, Lu D, Yao S, et al. The WNT receptor FZD7 is required for maintenance of the pluripotent state in human embryonic stem cells. Proceedings of the National Academy of Sciences. 2014;111(4):1409-14.
31. Price FD, Yin H, Jones A, van Ijcken W, Grosveld F, Rudnicki MA. Canonical Wnt signaling induces a primitive endoderm metastable state in mouse embryonic stem cells. Stem Cells. 2013;31(4):752–64.
32. Huang TS, Li L, Moalim-Nour L, Jia D, Bai J, Yao Z, et al. A Regulatory Network Involving β-Catenin, e-Cadherin, PI3k/Akt, and Slug Balances Self-Renewal and Differentiation of Human Pluripotent Stem Cells In Response to Wnt Signaling. Stem cells. 2015;33(5):1419–33.
33. Sokol SY. Maintaining embryonic stem cell pluripotency with Wnt signaling. Development. 2011;138(20):4341–50.
34. Davidson KC, Adams AM, Goodson JM, McDonald CE, Potter JC, Berndt JD, et al. Wnt/β-catenin signaling promotes differentiation, not self-renewal, of human embryonic stem cells and is repressed by Oct4. Proceedings of the National Academy of Sciences. 2012;109(12):4485-90.
35. Famili F, Brugman MH, Taskesen E, Naber BE, Fodde R, Staal FJ. High levels of canonical Wnt signaling lead to loss of stemness and increased differentiation in hematopoietic stem cells. Stem Cell Reports. 2016;6(5):652–9.
36. Zheng B, Jarugumilli GK, Chen B, Wu X. Chemical probes to directly profile palmitoleoylation of proteins. Chembiochem: a European journal of chemical biology. 2016;17(21):2022.
37. Kelly OG, Pinson KI, Skarnes WC. The Wnt co-receptors Lrp5 and Lrp6 are essential for gastrulation in mice. Development. 2004;131(12):2803–15.
38. Gadue P, Huber TL, Paddison PJ, Keller GM. Wnt and TGF-β signaling are required for the induction of an in vitro model of primitive streak formation using embryonic stem cells. Proceedings of the National Academy of Sciences. 2006;103(45):16806-11.
39. Kubo A, Shinozaki K, Shannon JM, Kouskoff V, Kennedy M, Woo S, et al. Development of definitive endoderm from embryonic stem cells in culture. Development. 2004;131(7):1651–62.

Figures

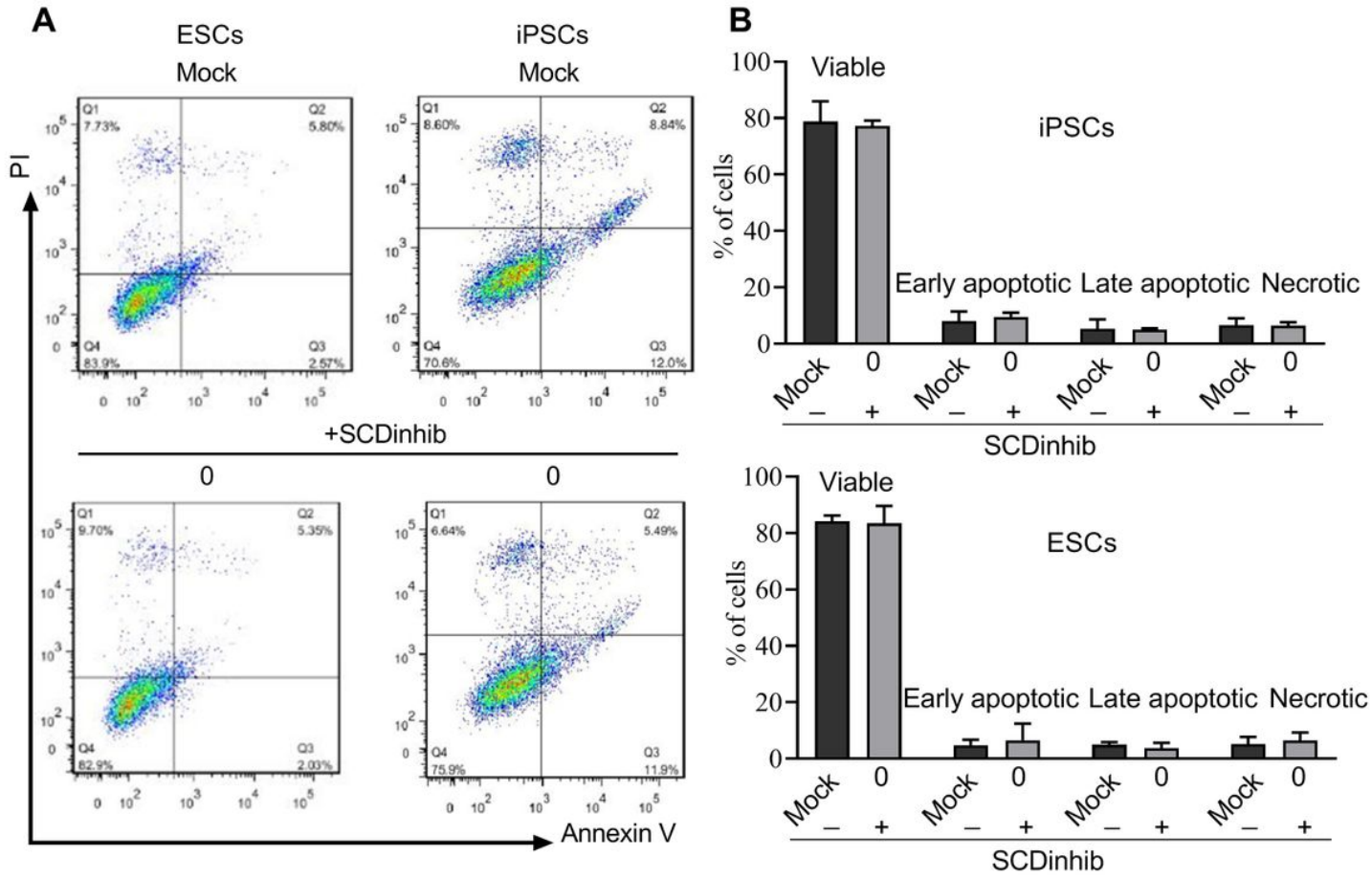

Figure 1

Flow cytometric analysis of pluripotent stem cells after treatment with the SCD1 inhibitor. (A) Representative flow cytometry dot plots showing four cell fractions: viable cells (annexin V-/PI-), early apoptotic cells (annexin V+/PI-), late apoptotic cells (annexin V+/PI+) and necrotic cells (annexin V-/PI+). The induced pluripotent stem cells (iPSCs) and embryonic stem cells (ESCs) were mock treated with DMSO (<0.05%, above) or treated with 25 nmol/L of SCD1 inhibitor (SCDinhib) at day 0 of differentiation (below) for 4 days. Cells were then harvested and evaluated for apoptosis and necrosis. (B) Quantification of cells in different groups.

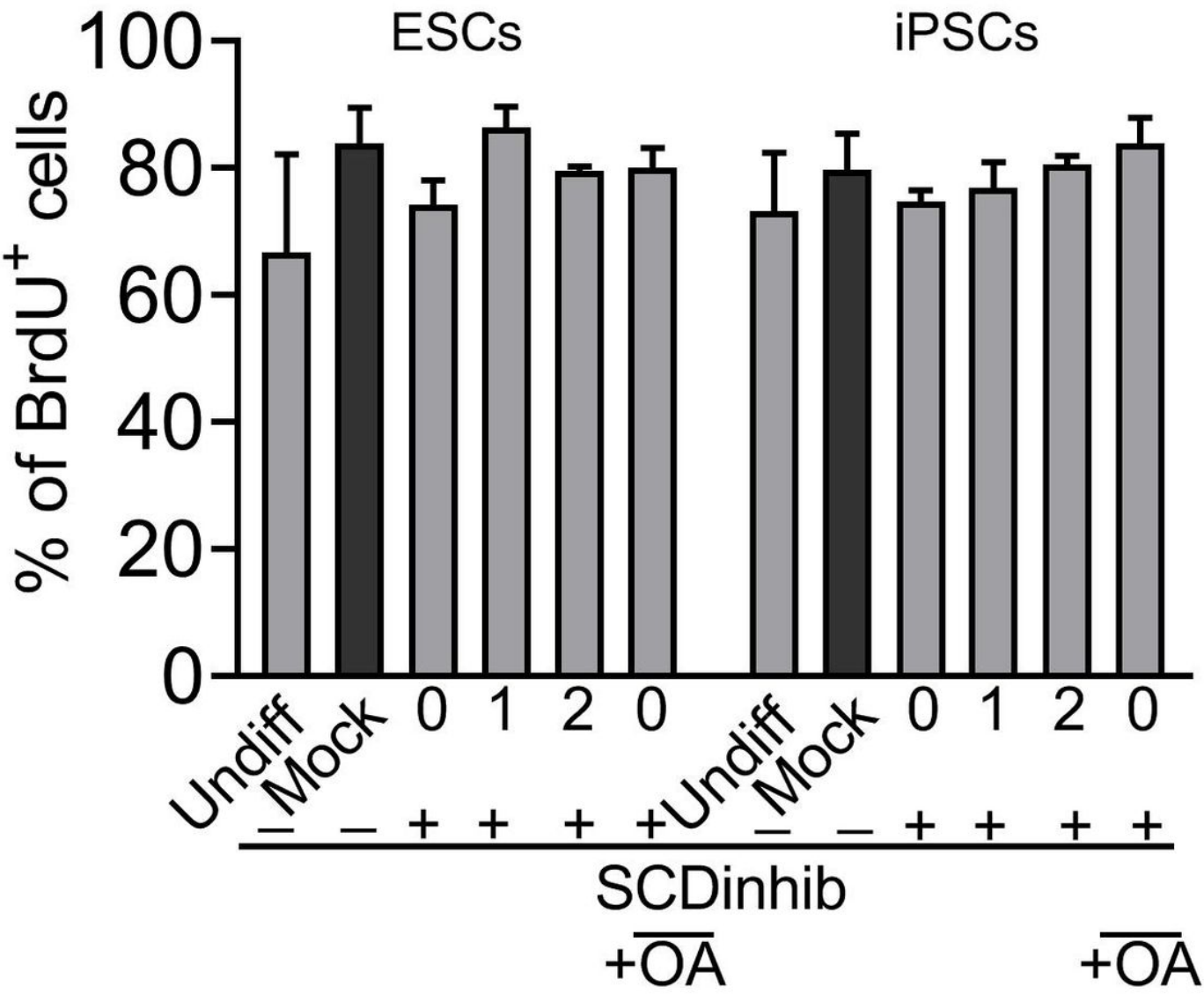

Figure 2

Cell growth determination using BrdU incorporation assay. The induced pluripotent stem cells (iPSCs) and embryonic stem cells (ESCs) were treated with SCD1 inhibitor (SCDinhib) alone at days 0, 1 or 2 (0, 1, and 2) of differentiation or in combination with oleic acid (OA) at day 0. Undifferentiated cells (Undiff) and cells treated with DMSO (<0.05 %, Mock) were served as background controls. The cells were harvested at day 4.

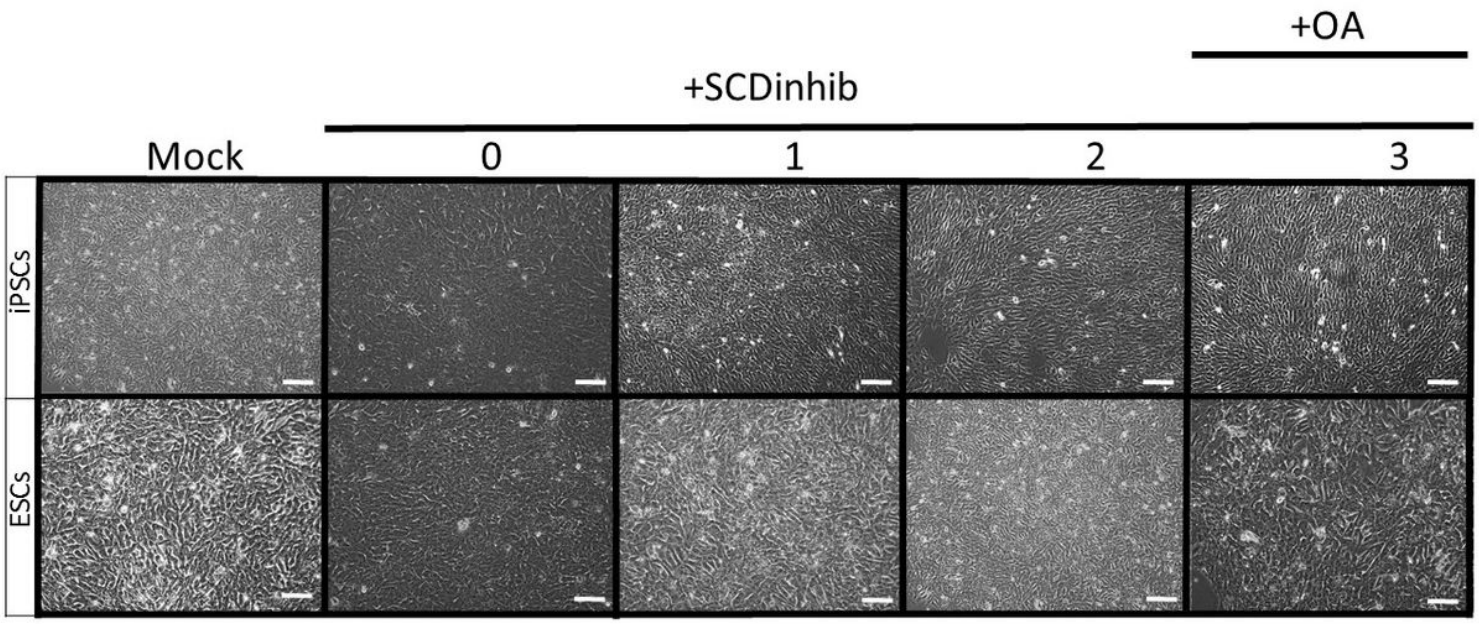

Figure 3

Phase contrast appearance of differentiated pluripotent stem cells treated with SCD1 inhibitor. SCD1 activity was suppressed at day 0, 1 or 2 (0, 1, and 2) of endodermal differentiation and imaged at day 4. Treatment of SCD1 inhibitor at day 0, but not at day 1 or 2 or with oleate at day 0, resulted in maintaining stemness morphology. Scale bar: 100 μm

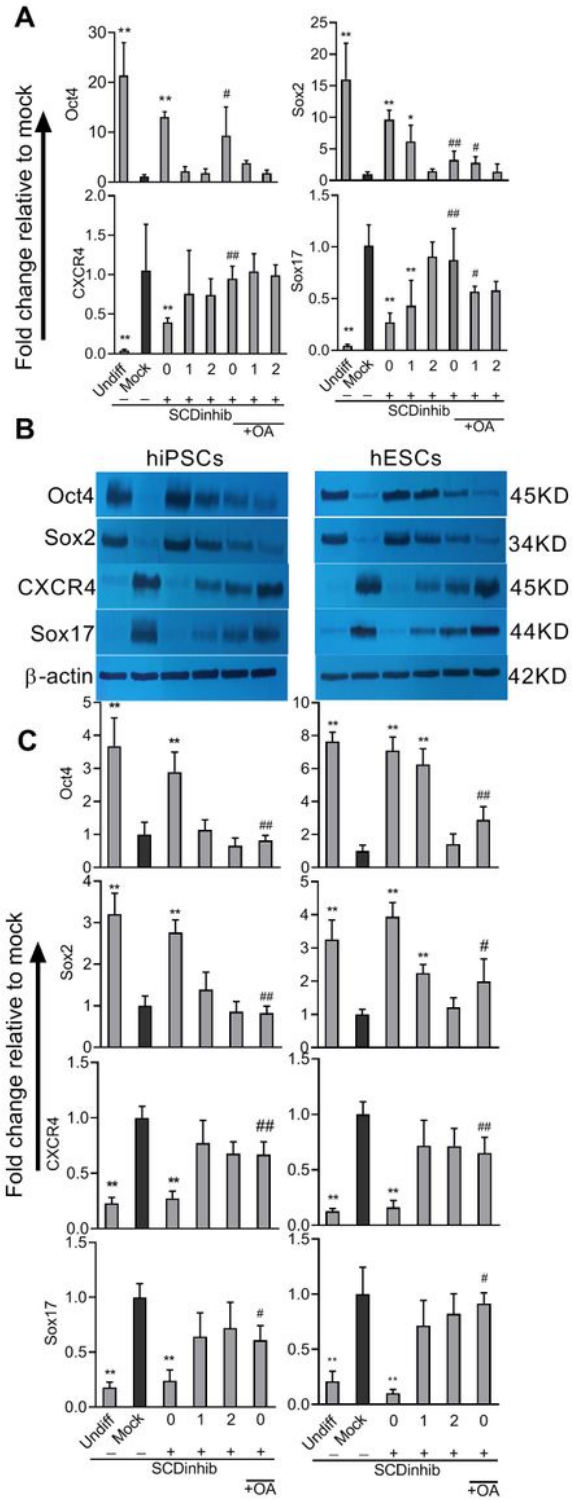

Figure 4

The expression of endoderm and stemness markers following the inhibition of SCD1 activity during induced differentiation. Cells were treated with SCD1 inhibitor (SCDinhib) alone at days 0, 1, or 2 (0, 1, and 2) of differentiation or in combination with oleic acid (OA) at day 0. Undifferentiated cells (Undiff) and cells treated with DMSO (<0.05 %, Mock) were served as background controls. The cells were harvested on day 4. The gene expression in iPSCs (A) and protein expression (representative Western blot

and quantification) (B) of the stemness markers Oct4 and Sox2 and endoderm markers CXCR4 and Sox17 were evaluated in the induced pluripotent stem cells (iPSCs) and embryonic stem cells (ESCs) using quantitative PCR and Western blot, respectively. (C) Quantification of protein expression in different groups. *p<0.05, **p<0.01 versus mock, #p<0.05, # #p< 0.01 versus the same day in SCDinhib.

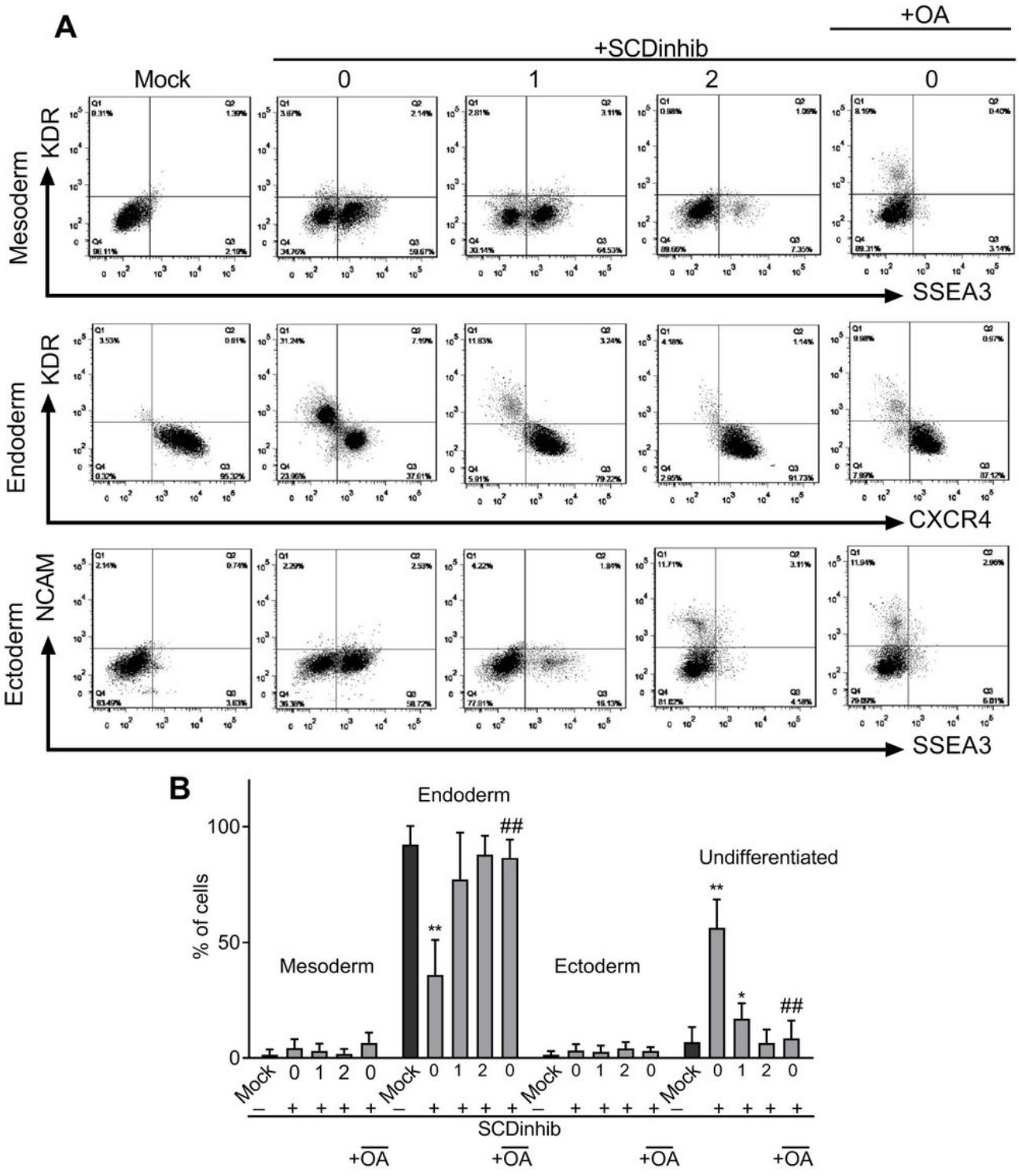

Figure 5

The germ layer markers following inhibition of SCD1 during endodermal differentiation of the induced pluripotent stem cells (iPSCs). Cells were induced to differentiate while treated with SCD1 inhibitor (SCDinhib) alone at days 0, 1, or 2 (0, 1, and 2) of differentiation or in combination with oleic acid (OA) at day 0. The cells were harvested on day 4 and analyzed using flow cytometry. (A) Representative flow cytometry dot plots of the dual staining pattern of mesoderm (KDR+, SSEA3-), endoderm (CXCR4+, KDR-), ectoderm (SSEA3+, NCAM+), and undifferentiated (SSEA3+, NCAM-) cells. (B) Quantification of flow cytometry results in different groups. (C) *p<0.05, **p<0.01 versus mock, #p<0.05, # #p< 0.01 versus the same day in SCDinhib.

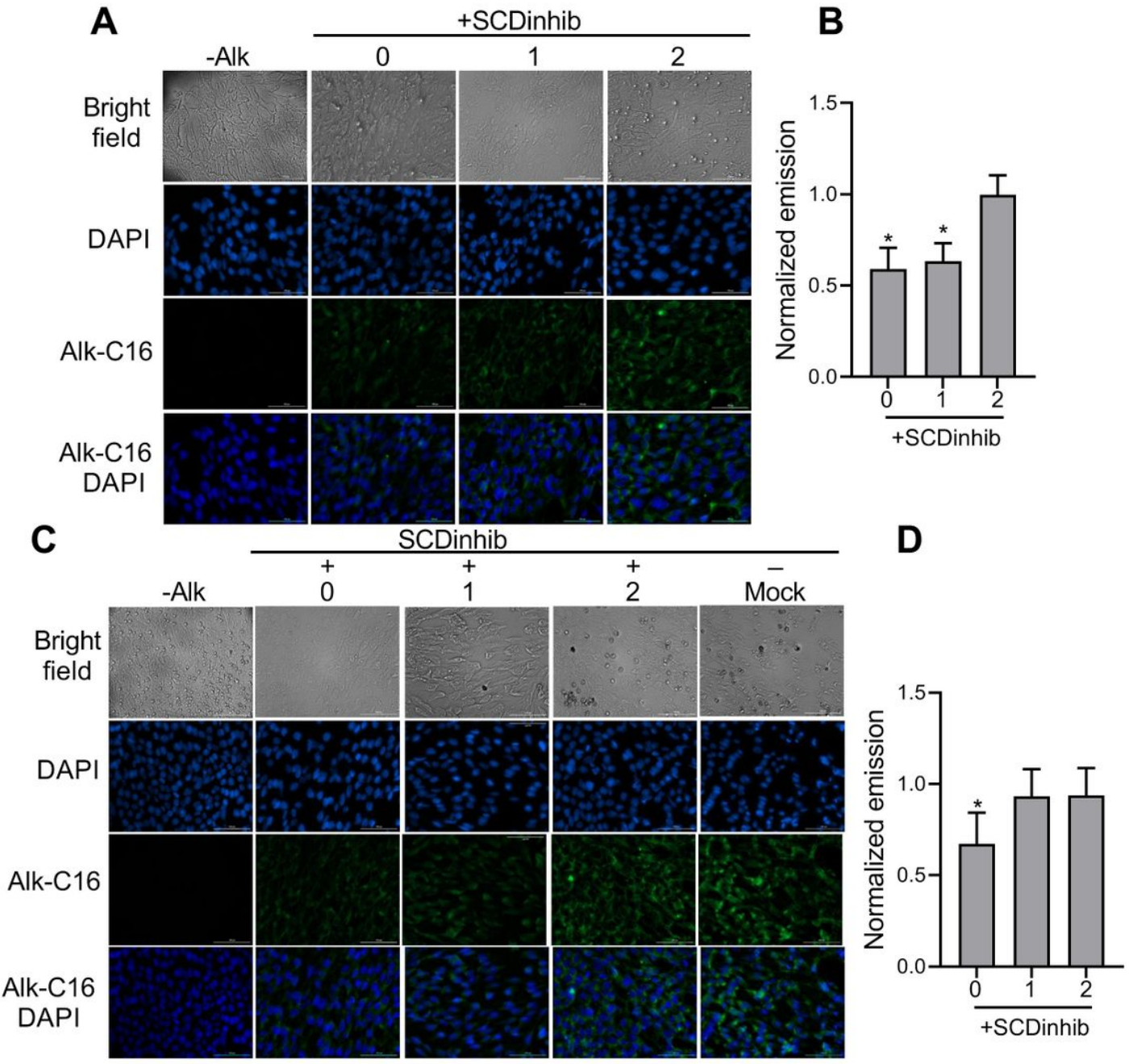

Figure 6

Click chemistry for labeling cellular proteins following inhibition of SCD1 during endoderm differentiation of the pluripotent stem cells. The induced pluripotent stem cells (iPSCs) and embryonic stem cells (ESCs) were induced to differentiate while treated with SCD1 inhibitor (SCDinhib) at days 0, 1, or 2 (0, 1, and 2). The click reaction was performed 24 h after each treatment. The cells were harvested on day 4. Representative fluorescence images of iPSCs (A) and ESCs (C) total protein acylation during endoderm differentiation. Quantification of fluorescence density in iPSCs (B) and ESCs (D) total protein acylation. The representative image of ESCs mock condition is shown in Figure S2. *p<0.05 versus mock. Scale bar: 100 μm.

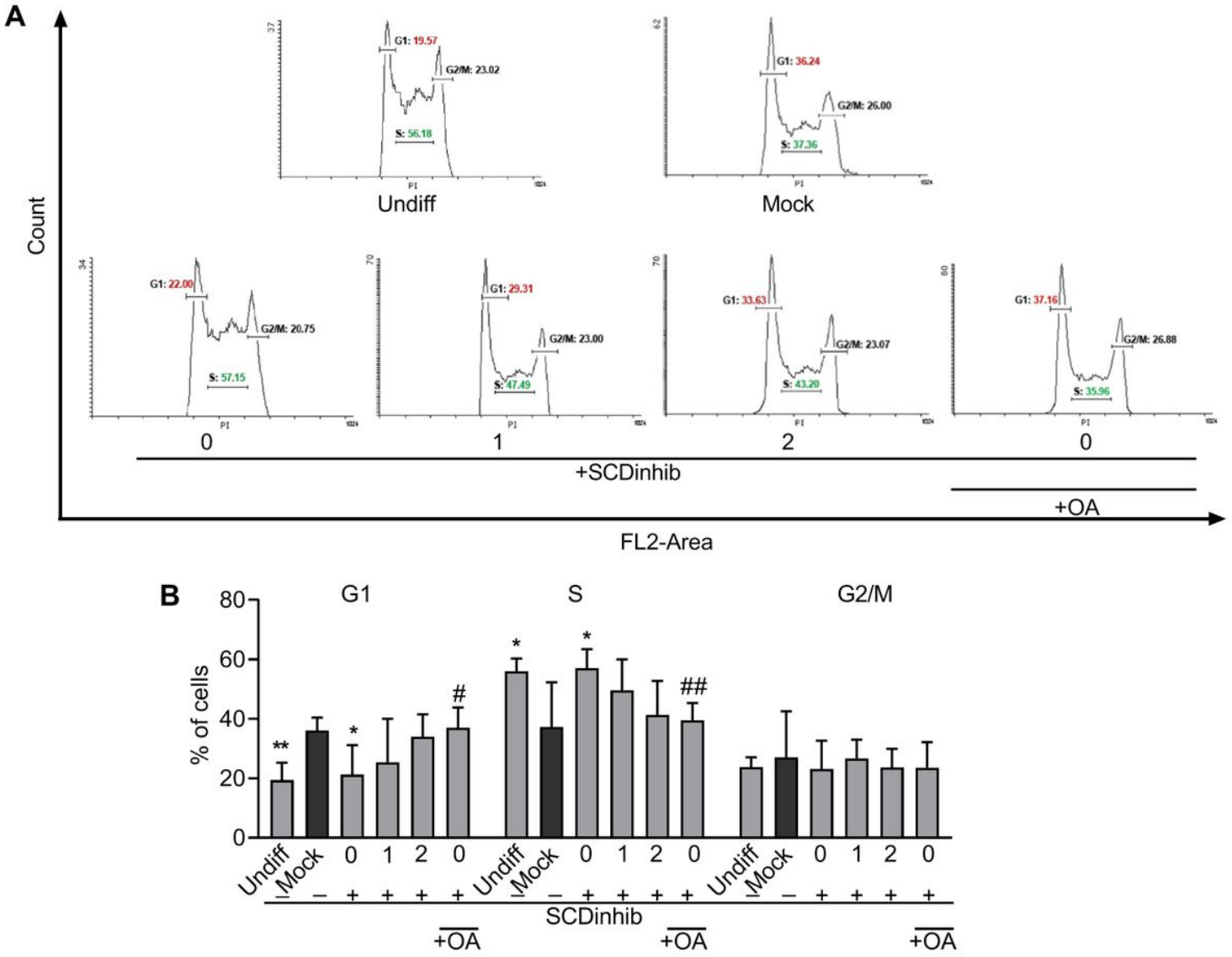

Figure 7

Cell cycle analysis following the inhibition of SCD1 activity during endoderm differentiation. The induced pluripotent stem cells (iPSCs) were treated with SCD1 inhibitor (SCDinhib) alone at days 0, 1, or 2 (0, 1, and 2) of differentiation or in combination with oleic acid (OA) at day 0. Undifferentiated cells (Undiff) and cells treated with DMSO (<0.05 %, Mock) were served as background controls. (A) representative flow

cytometers of cells. (B) Quantification of flow cytometry analysis. *p<0.05, **p<0.01 versus mock, #p<0.05, # #p< 0.01 versus the same day in SCDinhib.

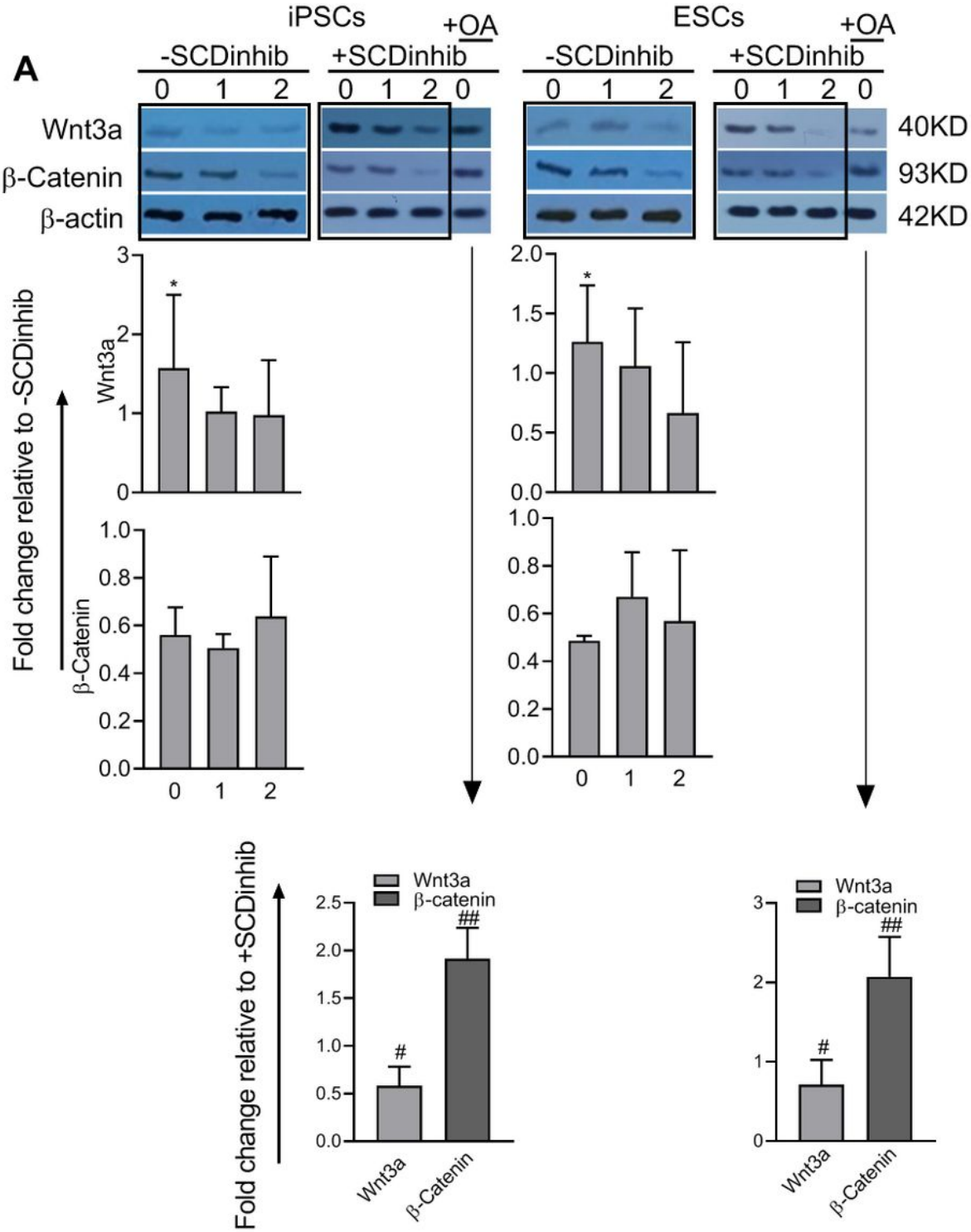

Figure 8

Analysis of Wnt signaling pathway following endoderm differentiation of pluripotent stem cells. The induced pluripotent stem cells (iPSCs) and embryonic stem cells (ESCs) were treated with SCD1 inhibitor (SCDinhib) alone at days 0, 1, or 2 (0, 1, and 2) of differentiation or in combination with oleic acid (OA) at

day 0. (A) The representative Western blot and the quantification of Wnt3a and β-catenin. *p<0.05 versus mock, #p<0.05, ##p< 0.01 versus the same day in SCDinhib.

Supplementary Files

This is a list of supplementary files associated with this preprint. Click to download.

- SupplementaryTable1.docx
- Fig.S1.jpg
- Fig.S2.jpg
- Fig.S3.jpg
- GraphicalAbstarct.png